

# We are IntechOpen, the world's leading publisher of Open Access books Built by scientists, for scientists

6,900

Open access books available

186,000

International authors and editors

200M

Downloads

Our authors are among the

154

Countries delivered to

TOP 1%

most cited scientists

12.2%

Contributors from top 500 universities



WEB OF SCIENCE™

Selection of our books indexed in the Book Citation Index  
in Web of Science™ Core Collection (BKCI)

Interested in publishing with us?  
Contact [book.department@intechopen.com](mailto:book.department@intechopen.com)

Numbers displayed above are based on latest data collected.  
For more information visit [www.intechopen.com](http://www.intechopen.com)



# Application of Virtual Instrumentation in Nuclear Physics Experiments

Jiri Pechousek  
*Palacky University in Olomouc,  
Czech Republic*

## 1. Introduction

The new way in the design of computer-based measurement systems can be seen in the use of up-to-date measurement, control and testing systems based on reliable devices. Digital signal processing (DSP) is used in all engineering areas, such as in nuclear physics experiments, to in order replace conventional analog systems and to build measurement and test systems with an easy configuration, user-friendly interface, and possibility to run sophisticated experiments. DSP systems are applied in nuclear physics experiments for their performance in both energy and time domain. Different programming techniques and instrument solutions are employed, and many commercially available digital oscilloscopes can be used in DSP systems.

Nowadays, nuclear DSP systems are commonly realized by the virtual instrumentation (VI) technique performed in LabVIEW graphical programming environment. The advantages of this approach lie in the use of (a) ready-to-start measurement functions (DSP algorithms), (b) instrument drivers delivered with measurement devices, and (c) in the possibility to improve a particular system when new algorithms, drivers or devices are available. With these opportunities, a system using the VI techniques and based on commercially available devices (USB, PCI, PXI etc.) can be driven by any suitable developed application. This application is then nearly "hardware platform independent".

Many papers concerning nuclear physics experiments have been published so far and in many of them, LabVIEW has been successfully applied. This chapter focuses on the description of the nuclear systems, which use the VI concept as much as possible, and in which a large number of system functions are performed in the software form.

As the first example, it can be mentioned the development of a computer-based nuclear radiation detection and instrumentation teaching laboratory system (Ellis & He, 1993), where the sophisticated setup of various devices is presented. Simulation and analysis of nuclear instrumentation using the LabVIEW is performed in ref. (Abdel-Aal, 1993). The high-performance digitizer system for high-energy and nuclear physics detector instrumentation employed in ref. (Kirichenko et al., 2001), is a time digitizing system in the VXI system. An FPGA-based digital and elaboration system for nuclear fast pulse detection (Esposito et al., 2007) is used for the direct sampling of fast pulses from nuclear detectors. Virtual instrumentation in physics described in (Tłaczala, 2005) presents applications for  $\gamma$ -rays intensity analyzer, data analysis and presentation. Models of

advanced nuclear physics experiments and measurements are presented as virtual laboratory with simulated nuclear physics experiments in (Tłaczala et al., 2008). The paper presents two simulated experiments that can be easily as well as remotely accessible ( $\gamma$ -energy determination and Mössbauer spectroscopy). Digital acquisition system (Belli et al., 2008) for digital pulse processing is applied to acquire data from n- $\gamma$  detectors. It is based on FPGA. The description of a versatile, computer-based  $\gamma$ -ray monitor is presented in ref. (Drndarevic & Jevtic, 2008) and a similar concept using VI based  $\alpha$ -particle spectrometer in ref. (Drndarevic, 2009). An auto-timing counts virtual instrument system with counter/timer module is presented in ref. (Yan et al., 2009). The development of an automated spectrofluorometer prototype, which is able to perform time-resolved fluorescence measurements, is described in ref. (Moreno et al., 2011). System is based on LabVIEW application and program controls the monochromator, and reads the information of the time-resolved detector signals measured by the digital oscilloscope. Fast pulse detection algorithms for digitized waveforms from scintillators (Krasilnikov et al., 2011) are implemented into the application that performs n- $\gamma$  pulse shape discrimination.

In the LabVIEW powered DSP system (Pechousek et al., 2011) the VI technique has been applied to develop a system which provides nuclear spectroscopic measurements such as amplitude and time signal analysis. The system is based on a high-speed digitizer, acquires data from two simultaneously sampled channels, and is fast enough to capture the pulses from different types of nuclear detectors. The system finds its application in the time coincidence measurement where two channels are used for the start and stop nuclear events registration. The VI techniques were also applied for the development of the fully-LabVIEW powered Mössbauer spectrometer (Pechousek et al., 2005, 2007, 2010, 2011). This system is based on the phenomena of the nuclear resonance absorption and emission of the  $\gamma$ -rays.

## 2. Virtual instrumentation in nuclear physics instrumentation

There are several types of radiation spectroscopies, such as  $\gamma$ -ray, X-ray, spectroscopy of charged particles (alpha, electron, proton, etc.), neutron, mass, time and others, that utilize different properties of radiation to study materials and particles (Ahmed, 2007; Gilmore, 2008). Today, each of these spectroscopic measurements can be based on DSP technique. The differences consist in the type of used detector and overall data analysis process. On the other hand, low-level DSP algorithms and methods for signal/pulse analysis can be similar. The standard structure of the DSP  $\gamma$ -ray spectroscopy system is depicted in Figure 1. The DSP algorithms can replace most of analogue modules.

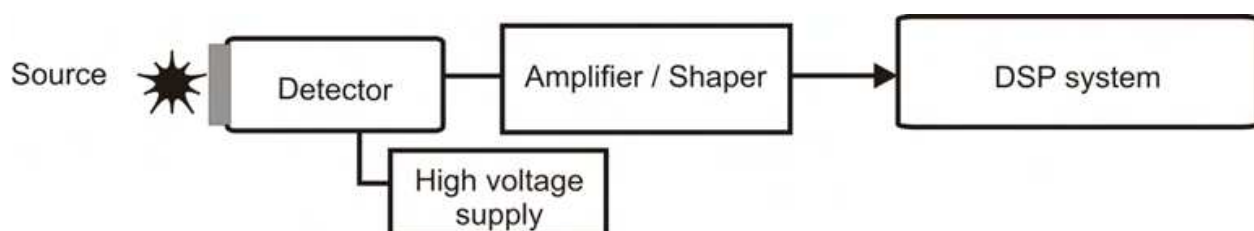


Fig. 1. Block diagram of standard DSP spectroscopy system.

Each DSP system has to use a device that digitizes an analog signal. A fast digital oscilloscope (digitizer) records the output signal from the radiation detector as an unprocessed signal or can acquire pulses coming through the signal amplifier or another preprocessing module. In the acquired signal, the pulse represents the nuclear event registration, and the amplitude of the peaks generally depends on the detected energy. The preamplifiers are used to amplify the low level signal and to match the detector and external circuit impedance. The typical acquired signal is shown in Figure 2.

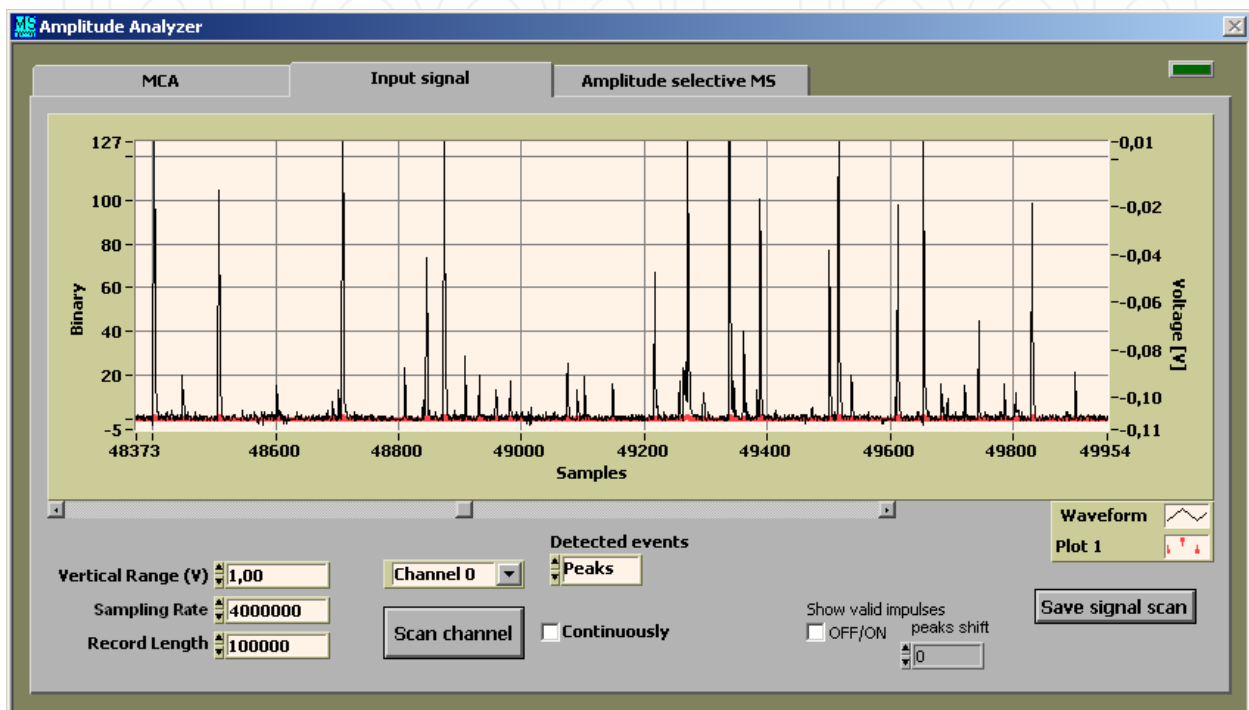


Fig. 2. Typical signal shape acquired from the nuclear detector.

## 2.1 Digitizing the signal from the detector

Data acquisition (DAQ) processes are performed digitally. There are two ways how to process data. Firstly, data are sampled (and transferred) by a digital oscilloscope, and acquired in a DSP program code. The second way is to sample data and acquire them by a programmable hardware (mostly by an FPGA) with DSP techniques implemented. Nowadays, many commercially available digitizers are frequently used either in the form of computer plug-in boards, or as stand-alone instruments connected to a computer via fast programming interface.

The digitizer discrimination properties are function of sampling rate and bit resolution. The 8-bit energy resolution is mostly used with very fast sampling rates in the order of  $GS\ s^{-1}$ . Today systems allow to use up to 16-bit resolution while achieving these sampling rates (Aspinall et al., 2009) for the best time resolution with fast detectors. The sampling rate used to digitize the detector output signal differs with the employed detector type. The sampling rates of about  $100\ MS\ s^{-1}$  are declared to be fast enough to capture the pulses from detectors for achieving the optimal pulse discrimination and to avoid the undersampling and signal aliasing. Hence, for most applications, a 10 ns time resolution is

sufficient to perform common time measurements (lifetime and other coincidence). Digitizer also produces accurate measurements if the analog bandwidth is wide enough and enables the signal to pass through without any attenuation (National Instruments, 2009a).

Currently, it is possible to increase the energy and time resolution by a fast digitizer or by a more advanced DSP technique. However, with increasing sampling rate and energy resolution, or using more robust algorithms, the dead-time of a spectrometer can increase due to a higher data transfer and processing, and, consequently, the overall counting rate can decrease.

### 2.1.1 Digital oscilloscopes

With up-to-date digitizers, special triggering and synchronization techniques can be exploited. These techniques allow to apply very sophisticated DAQ methods, where detector pulses can directly trigger DAQ process.

In this section, the use of technical and programming support for the NI-SCOPE instrument drivers and the National Instruments (NI) high-speed digitizers will be presented. The application of NI digitizers has been presented in ref. (Gontean & Szabó, 2011). In Figure 3, the types of NI digitizers applicable in various platforms are shown.



Fig. 3. USB, PCI, and PXI high-speed digitizers (National Instruments).

NI-SCOPE instrument driver is a set of software routines that control a programmable instrument. Each routine corresponds to a programmatic operation such as configuring, reading from, writing to, and triggering the instrument. Instrument driver functions can be divided in six categories – Initialize, Configuration, Action/Status, Data, Utility, and Close. As a part of this driver NI-SCOPE Soft Front Panel is also delivered, which is a software application for NI digitizers. When building a block diagram, it is necessary to apply several rules and recommendations, see NI-SCOPE Help (National Instruments, 2009a, 2010). Figure 4 shows the NI-SCOPE functions palette, where all subpalettes include the functions for digitizer control and data acquiring.

The function Initialize sets the driver and digitizer to a known state and establishes communication with the instrument. Configuration functions configure the instrument for performing a desired operation and, as a consequence, the instrument is ready to take measurements. Action functions cause the instrument to initiate or terminate the test and measurement operations. Status functions return the current status of the instrument. Data

functions include calls to transfer data to or from the instrument. Utility functions perform a variety of operations auxiliary to the most-used instrument driver calls. The Close function terminates the software connection to the instrument and deallocates system resources used during that instrument session (National Instruments, 2009a).

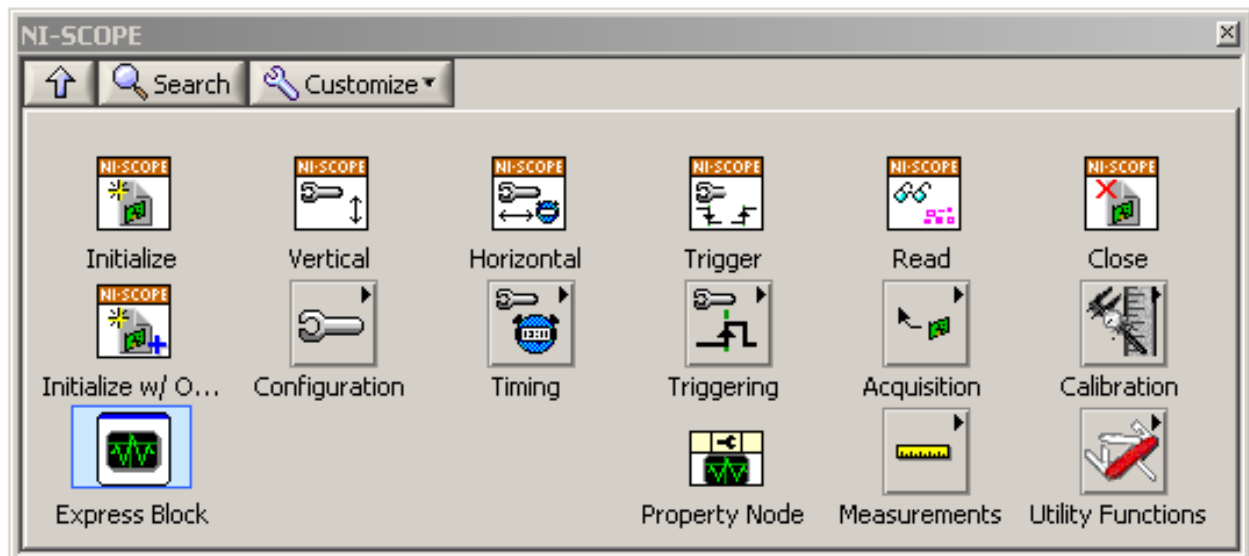


Fig. 4. NI-SCOPE palette.

The diagram in Figure 5 illustrates the basic programming flow for using NI-SCOPE functions in digitizer applications. The data flow is following. For any application, a session has to be open to establish the communication with the digitizer by using Initialize. After the initialization, the instrument is configured (vertical scale, horizontal scale, triggering options) and the DAQ process is started. Then, the data are read and transferred to DSP algorithms. When the program finishes, the DAQ process is aborted and the session has to be closed with Close.

The developed DSP module (depicted in Figure 5) was tested on PXI, PCI, and USB platforms, namely on NI PXI-5102 (8-bit, 20 MS s<sup>-1</sup>), NI PCI-5124 (12-bit, 200 MS s<sup>-1</sup>), and NI USB-5133 (8-bit, 100 MS s<sup>-1</sup>) digitizers. In this example, the amplified pulse coming from a detector is acquired with the niScope Fetch (poly) function, which retrieves data that the digitizer has acquired and returns a one-dimensional array of binary 8-bit values.

## 2.2 Signal processing - pulse shaping and amplitude measurements

Detectors realize the detection and measurement of radiation. An electronic detector uses a detection medium to generate an electrical signal when radiation passes through it. There are different types of radiation detectors depending on the interaction of radiation with the matter (Ahmed, 2007). The DAQ processes will be demonstrated on the signals acquired from scintillation detectors which are based on photomultiplier tube (PMT) with a common NaI:Tl scintillator of two different thicknesses, fast YAP:Ce scintillator, and slow gas filled proportional counter (GPC).

The NaI:Tl scintillator has a high light yield and a relatively long decay time of 230 ns. The YAP:Ce scintillator has a much lower light yield and a short decay time of 28 ns.



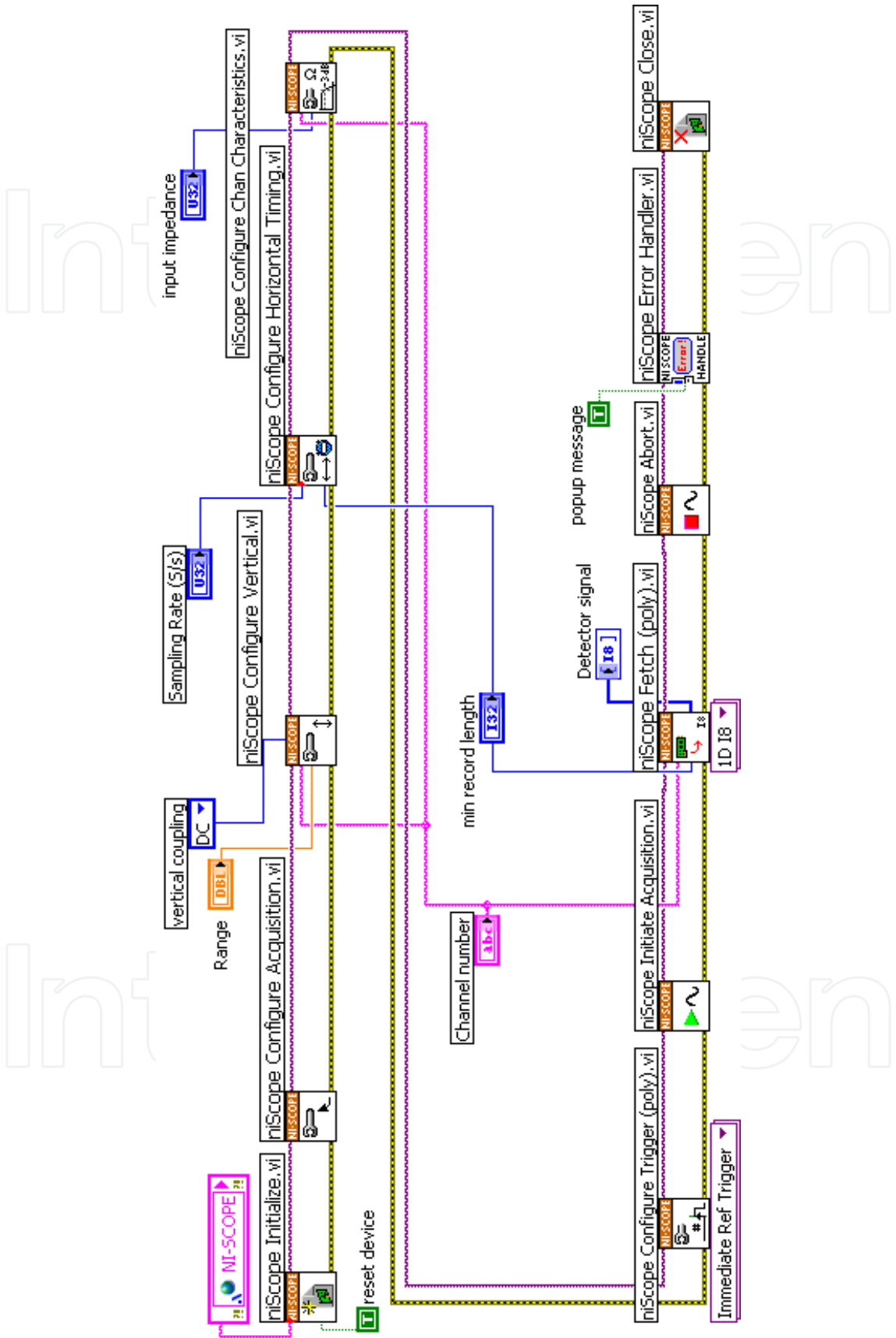


Fig. 5. LabVIEW code with NI-SCOPE driver functions.

It is suitable for the detection of a low energy  $\gamma$ -radiation. The optimal thickness for low energy  $\gamma$ -rays, 14.4 keV (emitted by  $^{57}\text{Co}$  source), are 0.15 mm for NaI:Tl and 0.35 mm for YAP:Ce, respectively (Kholmetskii et al., 1997). The PMT is used to detect scintillation photons. The result is an electric output pulse with amplitude large enough to be easily measured by a digitizer. In both cases, the low energy detectors are laboratory made with an integrated high voltage supply (Figure 6). The high energy  $\gamma$ -ray detector is the commercial detector (Scionix) with a NaI:Tl scintillator, the thickness 51 mm and 38 mm in diameter (Figure 6). The GPC detector is the Xenon/Methane filled detector suitable mainly for X-ray detection.



Fig. 6. High energy detector - upper, and low-energy detector - lower; and simply PMT.

The amplified signals acquired from two detectors with (a) YAP:Ce and (b) thick NaI:Tl scintillators are shown in Figure 7. The pulses from the particular detector are acquired, and the locations and magnitudes of their amplitudes can be obtained. The signals are obtained with the radioactive source  $^{57}\text{Co}$  and sampling rate of 200 MS  $\text{s}^{-1}$ .

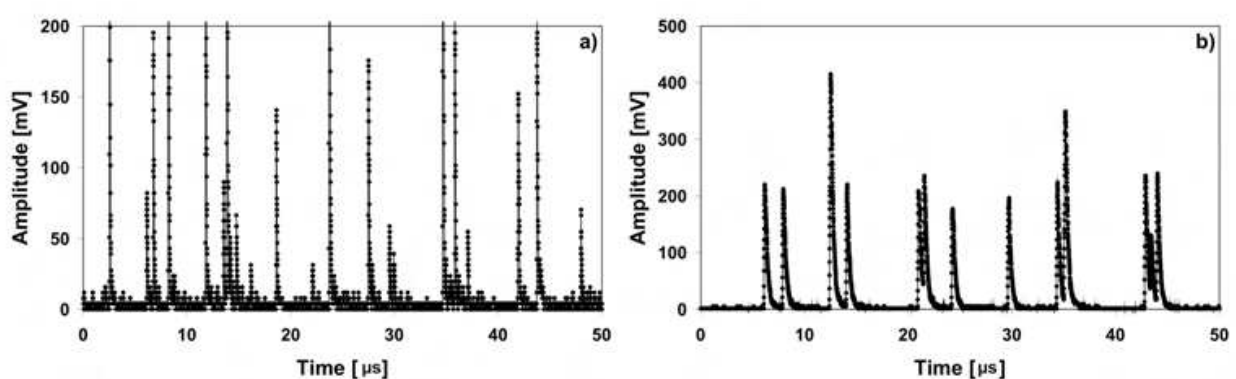


Fig. 7. Signals from a) YAP:Ce detector (14.4 keV) and b) thick NaI:Tl detector (122 keV).

Digitally implemented signal processing features (shaping, filtering, pulse validation, energy and time measurement, pulse shape analysis, noise reduction, pile-up rejection, amplitude multichannel analysis (MCA), etc.) can offer one DSP system for various types of



detectors. At this time, there are many DSP systems for the pulse shape analysis/determination. They are namely applied in a high counting rate of X-ray,  $\gamma$ -ray and/or nuclear particles.

Pulse shaping is used for increasing the signal to noise ratio and also for increasing the pulse pair resolution, hence, the commonly applied DSP method is a pulse pile-up correction. In the case of nuclear detectors, when high activity sources and detectors with a long pulse decay time are used, two or more events can be recorded as a single event. Various methods are used for the detection and either the correction or rejection of these pulses (Cosulich et al., 1992; Belli et al., 2008). The pile-up affects the counting rate, energy and time resolution of the spectroscopy system. Fast scintillators may be used for a pile-up rejection; however then, fast DSP systems have to be used. The innovative DSP algorithms for an optimal filtering, rise-time discrimination, and proper pulses correction are also used.

The DSP based amplitude analysis in LabVIEW can be developed with LabVIEW function Waveform Peak Detection VI (WPkD). The amplitude analysis process is controlled by several input parameters of WPkD (Figure 8). The amplitude values of the detected peaks are used for the pulse height analysis.

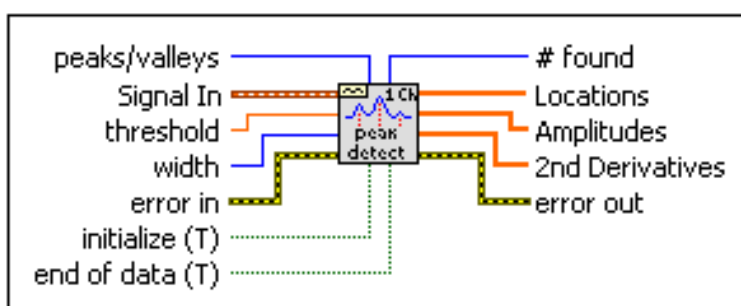


Fig. 8. Icon of Waveform Peak Detection VI.

WPkD function finds the location, magnitude of amplitude and the 2nd derivatives of the peaks in the detector signal. The threshold and width, input parameters, serve as separation tools of the true detector pulses from the noise. The threshold determinates the minimum value of the peak amplitude and the width determinates the minimum peak width according to the number of samples over the given threshold. WPkD is a software equivalent of the electronic pulse height analyzer, hence, the optimal treatment of the detector signal from the various types of detectors is achieved by DSP. The implementation of WPkD function in the block diagram is shown in Figure 9.

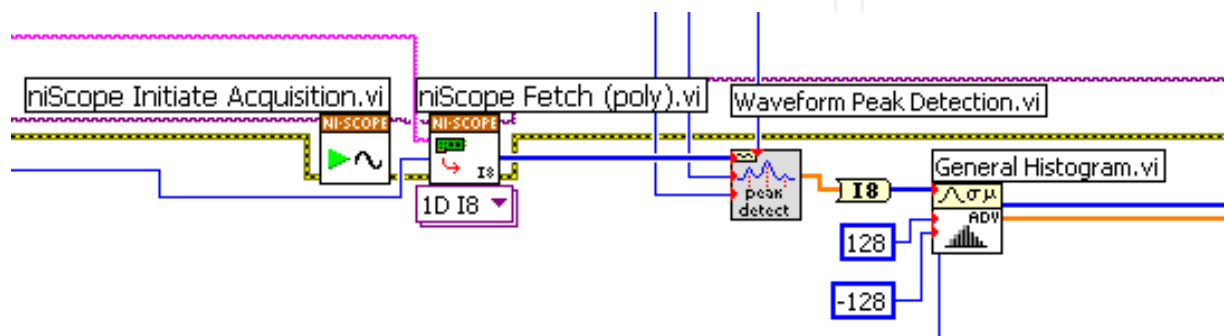


Fig. 9. Implementation of the WPkD function.

By changing the sampling rate, by means of the changes of the width and threshold parameters for peak validation in WPkD, the non-valid peaks rejection and signal noise reduction are performed. No pile-up correction/rejection is performed by this function. WPkD distinguishes the pile-up pulses, but their amplitudes are not corrected. In addition, few disadvantages of such function for the fast processing were found (Krasilnikov et al., 2011; Pechousek et al., 2007, 2011), and additional improvements, or new DSP algorithms were designed.

Another simple DSP module, called “discriminator”, checks whether the analog output signal is above a predefined threshold or not, and produces a digital output. The threshold values (voltages) can be adjusted through a front panel.

### 2.3 Signal analyzer and MCA application

The main part of the presented system is the commercially available digitizer NI PCI-5124, which uses up to 200 MS s<sup>-1</sup> real-time sampling. The digitizer is controlled by instrument drivers, as mentioned above, and called in the designed software application which performs all DSP functions. This digitizer was also used in  $\gamma$ -spectroscopy of high rate events (Yang et al., 2009) and in Mössbauer spectrometer designs (Pechousek et al., 2010). The <sup>57</sup>Co radiation source is used and typical pulses sampled by 200 MS s<sup>-1</sup> are displayed. The signals are acquired from the detectors connected with an amplifier. In Figure 10, the pulse shapes of three selected detectors are shown. The presented pulse shapes are the results of an average of one thousand pulses with the same amplitude.

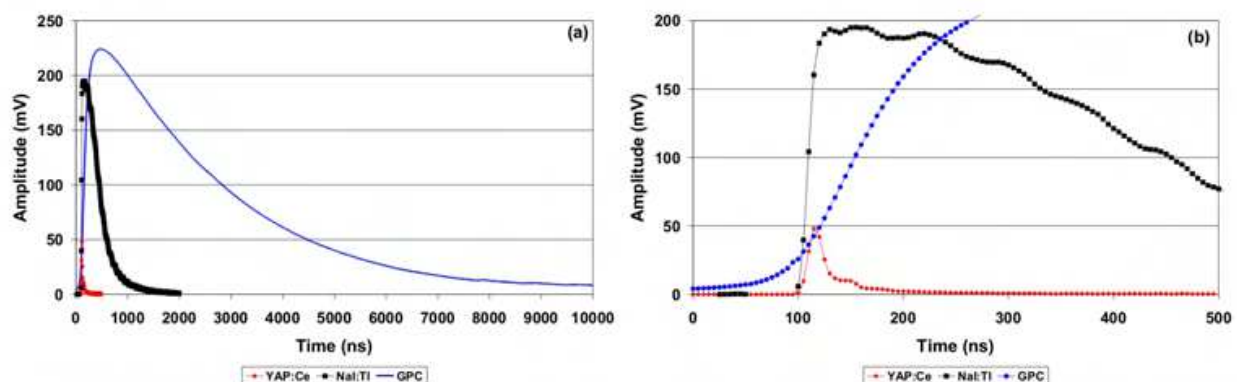


Fig. 10. a) The 14.4 keV pulses acquired from the detectors equipped with YAP:Ce scintillator (red) and GPC (blue) and 122 keV pulse acquired from the detector equipped with thick NaI:Tl scintillator (black), and b) the details of the rising parts of these pulses.

In Figure 10 (b), the common ringing in the pulses, mostly originating from the PMTs, is evident.

The most usual DSP method is the pulse height analysis preformed in MCA, which records the number of pulses in each pulse bin. In MCA, the channel number corresponds to the amplitude of a pulse, and the counting histogram is accumulated. Recently, DSP-MCA has been developed and system performance tested by us (Pechousek et al., 2011) on the nuclear detectors with very short time pulses (from 40 ns up to few microseconds), and in the range of low and high energies of X- and  $\gamma$ -rays. The front panel of the main application is shown in Figure 11, where negative pulses are acquired. The application code is based on the functions presented in Figures 5 and 9. Blue and red cursors in the MCA window (Figure 11) can be used to extract and analyze the pulses in a selected energy range. These cursors

are also used as the discrimination levels for the additional processing included e.g. in Mössbauer spectrometers.

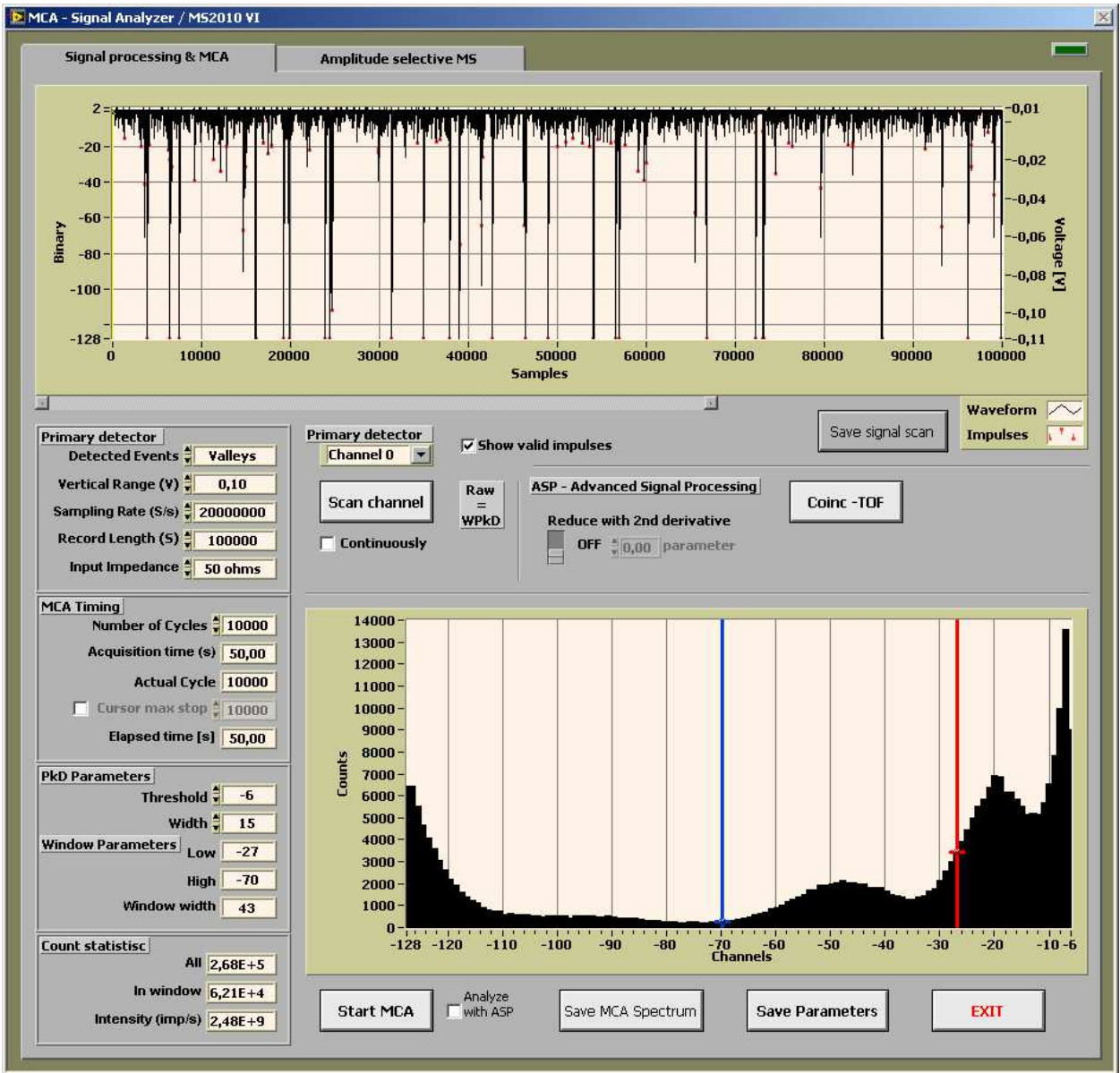


Fig. 11. Signal and Multichannel analyzer - front panel.

2.3.1 Improvement of MCA with high sampling rate

Four detectors employed for signal analysis and two  $\gamma$ -ray sources are presented in this part. For each detector, MCA was performed and the main photopeak positions were determined. In addition to  $^{57}\text{Co}$  source,  $^{137}\text{Cs}$  ( $\gamma$ -ray, 662 keV) source was also used. The MCA spectra were measured by means of the detector, amplifier, digitizer, and analyzed by the DSP with the WPKD.

As a first step, the detector signal was sampled with a low sampling rate (10 MS s<sup>-1</sup>) for establishing the standard values. This sampling rate is usable in classic MCA and slow coincidence systems, but it is still low for a precise MCA spectrum recording. In fast lifetime measurements, it is necessary to use a maximal sampling rate (time resolution) and,

therefore, the analysis with this sampling rate could be performed for the estimation of the influence on the MCA spectrum shape (energy resolution). Hence, the second value of the sampling rate was chosen to be of  $200 \text{ MS s}^{-1}$ . The MCA energy spectra of X- and  $\gamma$ -radiation emitted by  $^{57}\text{Co}$  and  $^{137}\text{Cs}$  sources are shown in Figure 12, where black line belongs to a low sampling rate and red line to a high sampling rate, respectively.

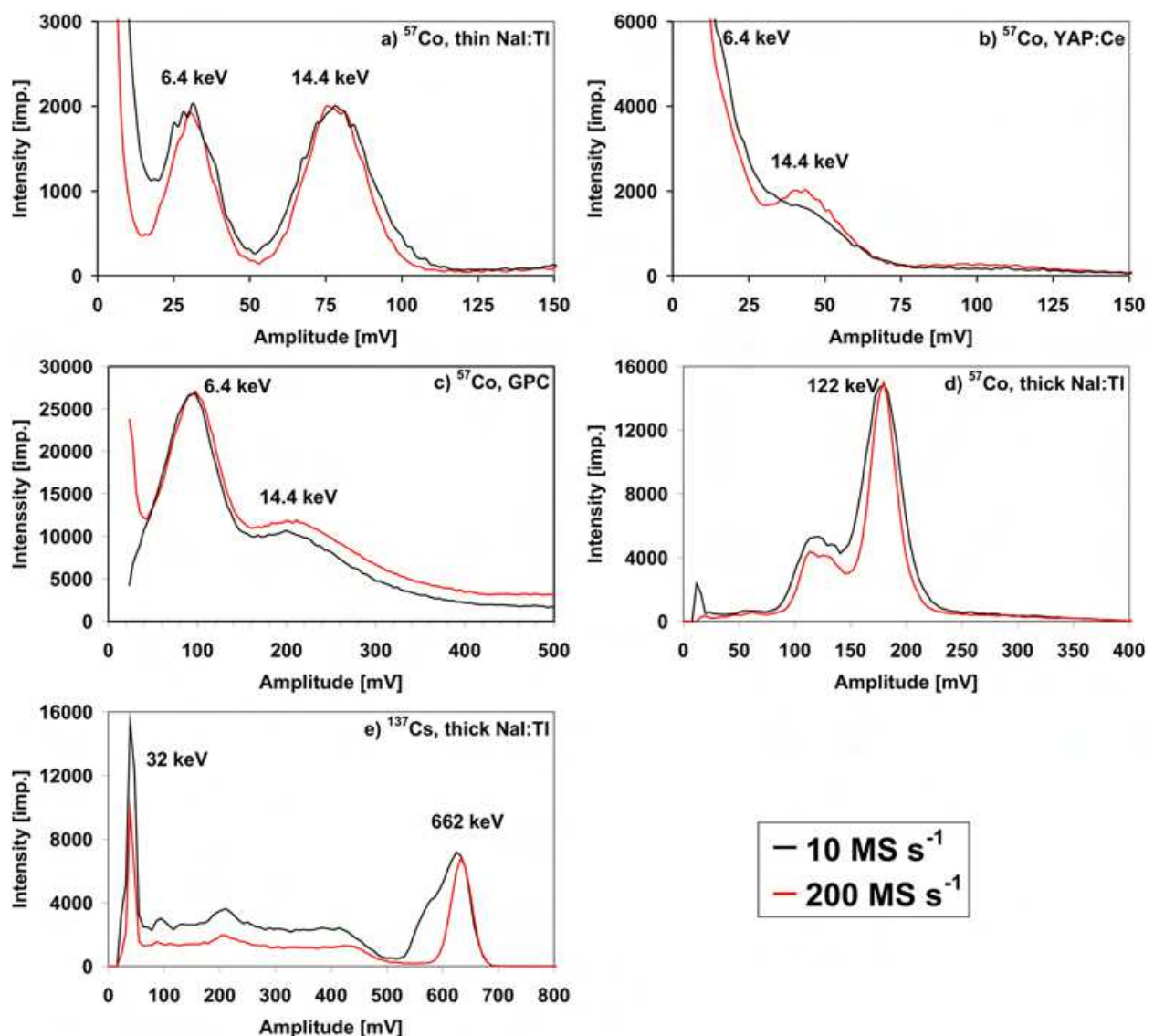


Fig. 12.  $^{57}\text{Co}$  MCA spectra for a) thin NaI:Tl, b) YAP:Ce scintillators, c) GPC, d) thick NaI:Tl scintillator, and e)  $^{137}\text{Cs}$  MCA spectrum for thick NaI:Tl scintillator. Signal is acquired at  $10 \text{ MS s}^{-1}$  and  $200 \text{ MS s}^{-1}$  sampling rate.

When the detector or source was changed from one to another, the distance was adjusted to achieve the reasonable counting rates and to minimize the occurrence of pile-up events. Figure 12 shows the energy resolution improvement for all photopeaks except the GPC detector, in which case a significant improvement is not evident. Furthermore, in the range of high energy impulses, another significant improvement is observed due to a better interleaving of the pulses. The  $10 \text{ MS s}^{-1}$  sampling rate is quite underlimited for the YAP:Ce coupled detector. Generally, the improvement for fast detectors and high energy regions is the most visible, due to the better recognition of the rising part of a observed pulse.



## 2.4 Time-of-flight and coincidence techniques

In common time-resolved coincidence nuclear systems, two different detectors are used in order to detect different photon energies emitted from the radioactive source, when a radioactive decay is studied. Similar methods are used i.e. in the time-resolved fluorescence system (Moreno et al., 2011) estimating the intrinsic fluorescence decay.

The system published in ref. (Pechousek et al., 2011) is suitable for nuclear coincidence measurements as the nuclear excited state half-life determination, where two DAQ channels are necessary. The first channel can detect the start nuclear events and the second channel the stop events. Both channels are sampled by the highest sampling rate. When the short-lived excited states are analyzed, time-of-flight (TOF) values has to be determined with the highest accuracy. The 200 MS s<sup>-1</sup> sampling rate is used for precise MCA and time-resolving measurements and the system is then sensitive to decay lifetimes from tens of nanoseconds. In Figure 13, a block diagram of the above discussed system is shown.

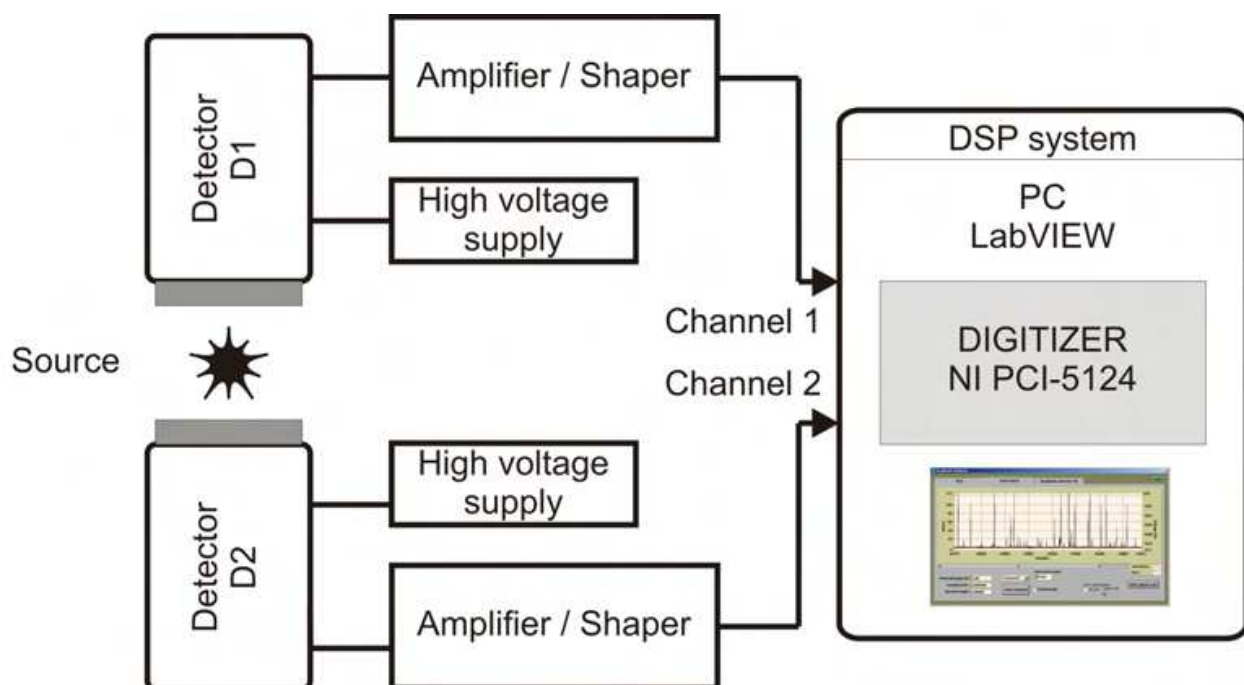


Fig. 13. DSP system for time-resolved nuclear spectroscopy.

In time-resolved spectrometry, the TOF value determines when a photon or particle arrives into the detector. The time accuracy of the measurement system depends on the properties of the detector and the type of electronics processing the signal. TOF measurement offers the possibility to perform coincidence and anticoincidence nuclear experiments. There are several analog timing methods (leading edge timing, crossover timing, constant-fraction timing, first photoelectron timing) implemented in DSP (Abdel-Aal, 1993; Aspinall et al., 2009). In one of them, the pulse starting time is interpolated from the samples of the pulse rise and a digital leading-edge discriminator (LED) determines the TOF value. The TOF then represents the time at which the pulse crosses the threshold (discrimination level). The LED is a simply implemented timing method usable mainly when similar pulses shapes in a signal stream occur. Therefore, the developed DSP system with the TOF-LED technique can be used with various types of detectors. The description of the LabVIEW LED is given in ref.



(Pechousek et al., 2011). The TOF algorithm development and its application in the coincidence measurement were carried out. The TOF calculation is depicted in Figure 14. The code has to distinguish between the maximum value position (from WPkD) and the beginning of the pulses.

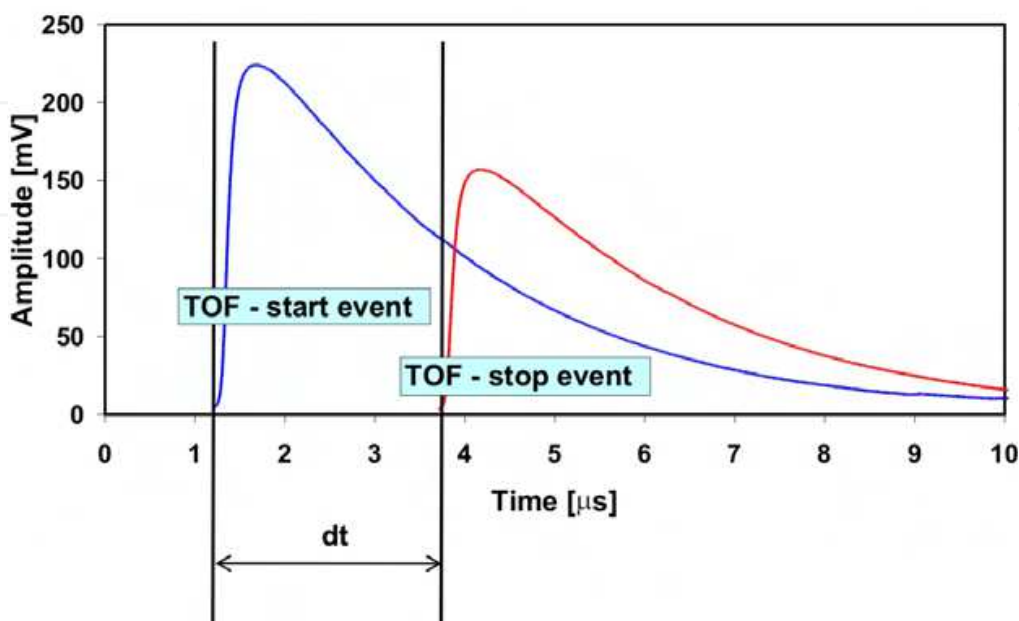


Fig. 14. Practical behavior of the TOF procedure.

As mentioned above, when using a code with the original WPkD function, only the valid peaks are recognized. However, problems arise for high-rate sampling and therefore, DSP-TOF improvement is necessary. With a high-rate sampling, the peak location is sometimes found out of the pulse-maximum position. This error-shift negatively affects time resolving measurements, and has to be reduced for a precise nuclear coincidence measurement by modifying the WPkD algorithm with adding the TOF determination. The presented modified TOF-resolving method is applicable for various detectors and is independent on the pulse rising time (Pechousek et al., 2011).

#### 2.4.1 Lifetime coincidence measurement

The presented DSP system is typically applied in the coincidence measurement where the lifetime of the excited nuclear state can be measured by the registration of X- $\gamma$ , or  $\gamma$ - $\gamma$  cascade. In this section, the lifetime coincidence measurement of  $^{57}\text{Fe}$  14.4 keV excited state is presented. The registrations of two events are acquired with two different detectors optimized for given energies. In the case of  $^{57}\text{Co}$  source, it decays by an electron capture to the excited state of  $^{57}\text{Fe}$  (136 keV) which deexcites thorough the 122 keV and 14.4 keV states to the ground state. The 14.4 keV excited state has a half-life of 98.3 ns (Dickson & Berry, 1986).

In accordance with Figure 13, the first detector (D1) detects 122 keV  $\gamma$ -photons (thick NaI:Tl) as start events and the second detector (D2) detects 14.4 keV  $\gamma$ -photons (YAP:Ce or thin NaI:Tl) as stop events. The coincidence intervals, calculated with TOF code, have been accumulated into the histogram, and are shown in Figure 15.

Each channel of the DSP system was configured individually to detect relevant start and stop events. The value of the half-life was estimated to be  $98.9 \pm 0.3$  ns.

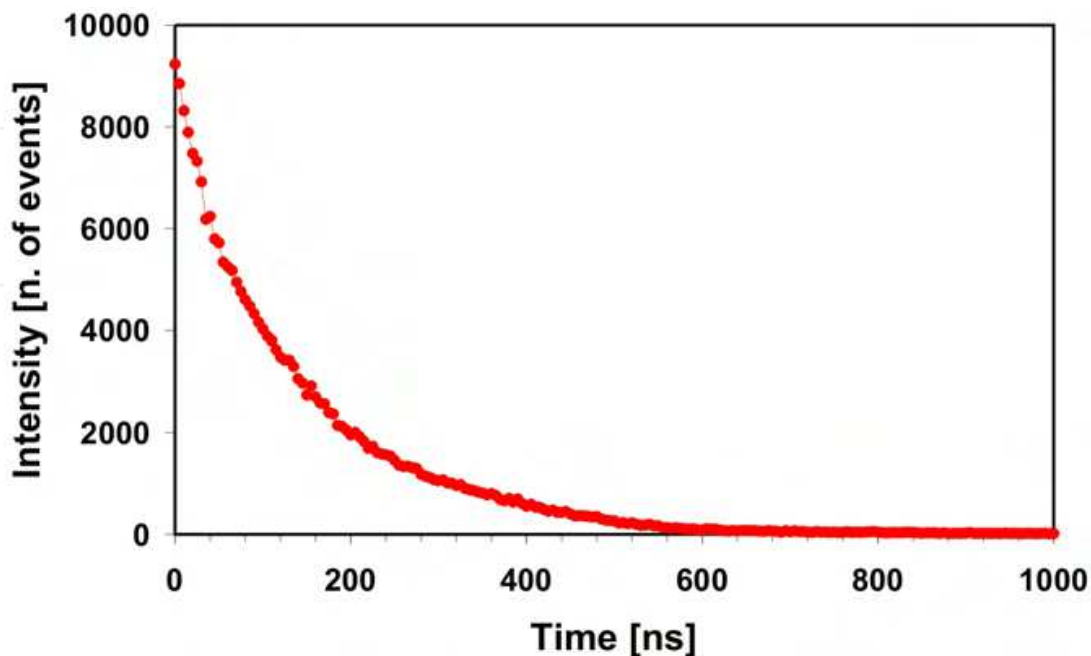


Fig. 15. Lifetime measurement of the 14.4 keV excited state in  $^{57}\text{Co}$  source.

### 3. Additional DSP methods in nuclear systems performed by VI

Acquiring data from a detector is the most common process in the nuclear systems. Additionally, various methods are used in other different spectroscopies. For instance, one method can be the generation of an analog signal (waveform) for controlling a particular device. Hence, synchronizing such DAQ processes with detector signal digitizing becomes necessary. This is described in the text below.

#### 3.1 Function generators

Different analog output devices are used. The function generator device with its instrument drivers delivered will be described. The examples presented below have been established with the NI 5401 (12-bit, 40 MS s<sup>-1</sup> update rate) function generator. This function generator features also the Real-Time System Integration (RTSI) or PXI trigger bus for routing the trigger signals in the PCI or PXI system to synchronize other DAQ processes. The NI-FGEN instrument driver is used in NI 5401 applications and the Soft Front Panel (SFP) can be employed to interactively generate waveforms with NI the signal generators module, in a similar way as with stand-alone instruments.

The diagram in Figure 16 shows the general programming flow for applications using NI-FGEN driver. Details are presented in LabVIEW NI-FGEN Help (National Instruments, 2004, 2009b).

This instrument driver is used in a similar way as the above mentioned NI-SCOPE driver. After the initialization and configuration processes, the signal generation is started. At the end of the generation, the abort function is called and the instrument session is closed.

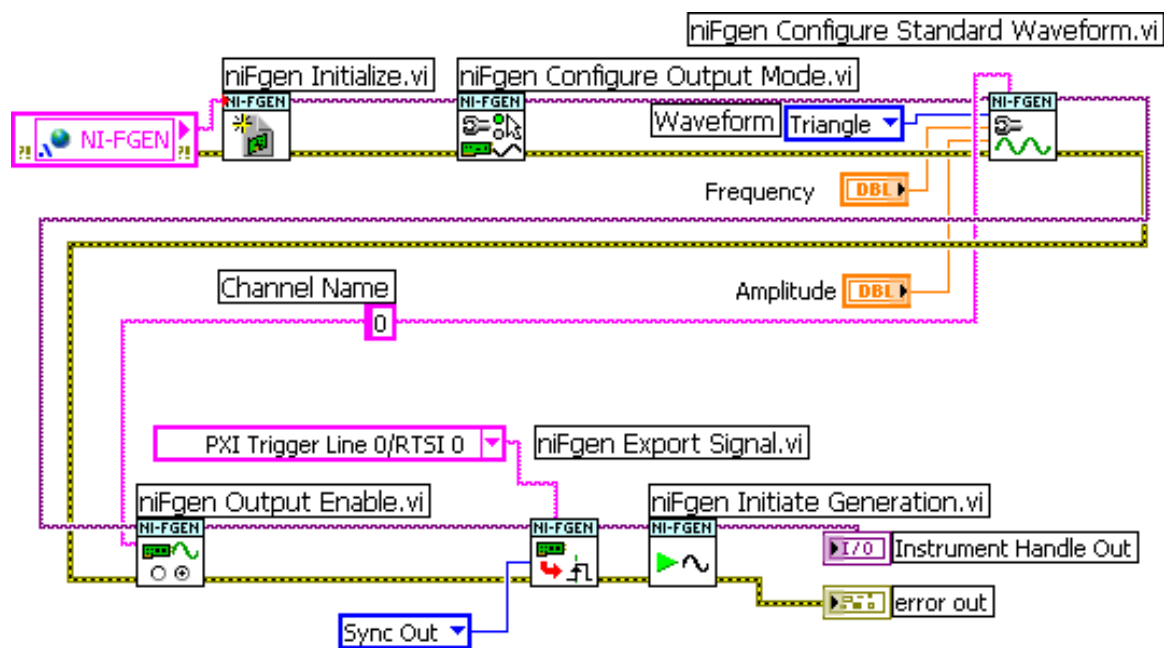


Fig. 16. Data flow for NI-FGEN application.

3.2 Synchronization and triggering techniques implemented via RTSI bus

If an application requires more than two DAQ devices, it is possible to synchronize these devices on all platforms using digital triggers. RTSI (Real-Time System Integration) bus is employed to share and exchange timing and control signals between multiple boards. The RTSI bus cables are short, 34-conductor ribbon cables equipped with two to five connectors linking together a group of boards. Figure 17 shows an example of an extended five-board cable setup.

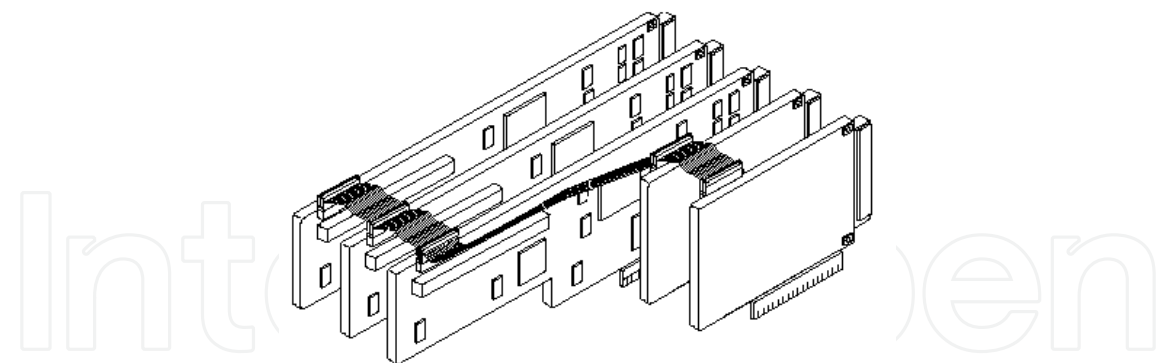


Fig. 17. RTSI bus used for synchronization of PCI devices (National Instruments, 2010).

The PXI system uses the PXI trigger bus that includes the RTSI bus and is linked to all slots in the chassis. Other devices can use the PFI (Programmable Function Interface) digital triggers on the I/O connector. Synchronization and triggering are commonly used in more sophisticated measurements, where one or more DAQ processes relate with other processes. Such a type of combination is common in applications where one device works as a master (generates signals) and the other device works as a slave (waits for trigger). In the VI concept, it is easy to build such a system and the exchange the working mode of these devices.

A trigger is a signal that initiates one or more instrument functions. The trigger basic types are digital, software, or analog, and can be derived from the attributes of a signal being acquired, such as the level and slope of the signal. Triggers can be internal (software-generated) or external. External triggers allow synchronizing the hardware operation with an external circuitry or other devices. There are several types of triggering, and each kind of triggering uses a different NI-SCOPE or NI-FGEN Configure Trigger function (National Instruments, 2009b, 2010).

For instance, in the computer-based modular Mössbauer spectrometer (Pechousek et al., 2010), there are two main parts; the first one is a computer with the NI 5102 digitizer, and the second, the NI 5401 function generator controlled by VI. Their synchronization is provided by the RTSI bus or PXI Trigger bus. The function generator generates a velocity signal on its ARB OUT output. On the SYNC OUT output, a trigger signal is available for the synchronization of other devices (the routing of this signal is shown in Figure 16). This is used in the internal RTSI bus and triggers the DAQ process in the digitizer. In the case of USB devices, it can be generated externally by the digital output signal available in the multifunction devices.

3.2.1 Triggering with NI-FGEN

When triggering a signal generator, it is possible to select the type of the trigger, trigger source, and trigger mode. For instance, the function generator works as a master, and except the periodic analog signal, it generates the digital trigger signal with the same frequency on the SYNC OUT output. This signal will be routed on the RTSI bus line by the function of *niFgen Export Signal VI* (see Figure 18) to control other devices. This function routes signals (clocks, triggers, and events) to the specified output terminal, i.e. the RTSI connector.

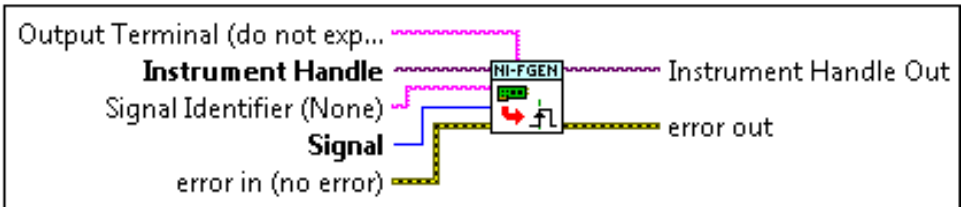


Fig. 18. Function *niFgen Export Signal VI* used to route the trigger signals.

The SYNC OUT signal is normally exported on the SYNC\_OUT front panel connector.

3.2.2 Triggering with NI-SCOPE

With NI-SCOPE triggering functions, the trigger can transfer a device from a nonsampling into a sampling state, then the device starts acquiring data. The function which configures the digitizer for different types of triggering is *niScope Configure Trigger (poly)*, see Figure 19.

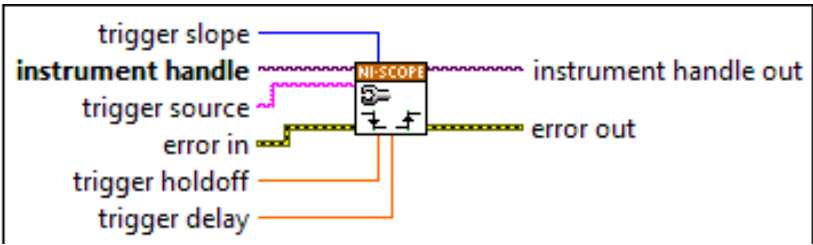


Fig. 19. Function *niScope Configure Trigger (poly)* used to trigger the digitizer.

After initializing an acquisition, the digitizer waits for the start trigger which is configured through the Start Trigger Source property. The default setting is “immediate”. Upon receiving the start trigger, the digitizer begins sampling pretrigger points. After the digitizer finishes sampling pretrigger points, the digitizer waits for a reference (stop) trigger that is specified by a Configure Trigger VI. Upon receiving the reference trigger, the digitizer finishes the acquisition after completing posttrigger sampling (National Instruments, 2010). The configuration of the digital and analog triggers with NI-SCOPE is shown in Figure 20.

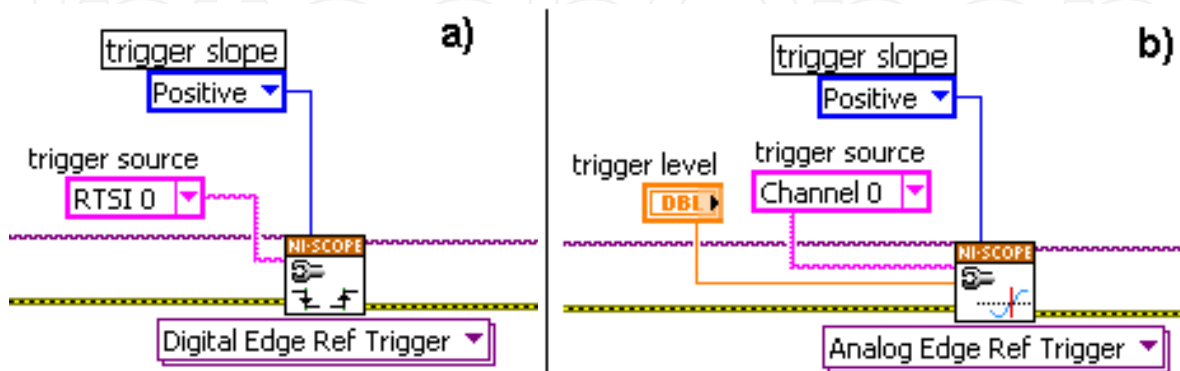


Fig. 20. Types of NI-SCOPE triggers a) digital and b) analog.

In the case of digitizers, analog triggers set at one DAQ channel can trigger the second channel (Figure 20 b), which is used in time resolved measurements. Analog triggers in digitizer applications are commonly used in time-resolved spectroscopies, in which two DAQ channels are used. This technique has been described in the previous section - the start event channel triggers the stop event channel.

#### 4. Mössbauer spectroscopy

In this section, methods for pulse processing, movement control and DSP synchronization will be presented and demonstrated on the Mössbauer spectrometer construction. All the tasks use DSP abilities of LabVIEW system running in the main computer, and the former single-purpose spectrometer units were replaced by DAQ modules. Hardware solution is based on DAQ devices working on the USB, PCI or PXI platform controlled by the main application running on the personal computer or PXI controller. Final application allows, in addition to Mössbauer spectra accumulation, the detailed analysis of the acquired detector signal in energy and time domains, and also to tune the velocity driving system separately. This concept can be used with all common spectrometric benches with different velocity transducers, radioactive sources and  $\gamma$ -ray detectors.

Mössbauer spectroscopy represents an essential tool for the investigation of specific elements-containing materials (Fe, Sn, Au ...) as its local probing capability. It allows to determine and quantify different atomic surrounding, magnetic states and in-field magnetic arrangements of magnetic moments, conveying thus structural and magnetic information. In addition, Mössbauer spectroscopy is highly element selective and allows identifying the desired component even if it exists in a very small amount in the mixed sample.

The Mössbauer effect is based on recoilless nuclear emission and resonant absorption of  $\gamma$ -rays in the sample, and the Mössbauer spectra acquisition is performed by the  $\gamma$ -ray intensity measurement together with the precise radioactive source motion control. The Mössbauer spectrum is dependency between radioactive source velocity and the detected  $\gamma$ -



ray intensity. This experimental technique is a frequently used tool in many areas of research such as physics, chemistry, biology, metallurgy etc.

#### 4.1 Spectrometer configuration

The standard structure of the Mössbauer spectrometer is depicted in Figure 21, where most of these blocks could be replaced by the DSP algorithms. The LabVIEW programming environment allows realizing such system with minimum single purpose electronic devices. The typical Mössbauer spectrometric bench is shown in Figure 22 (for room temperature measurements).

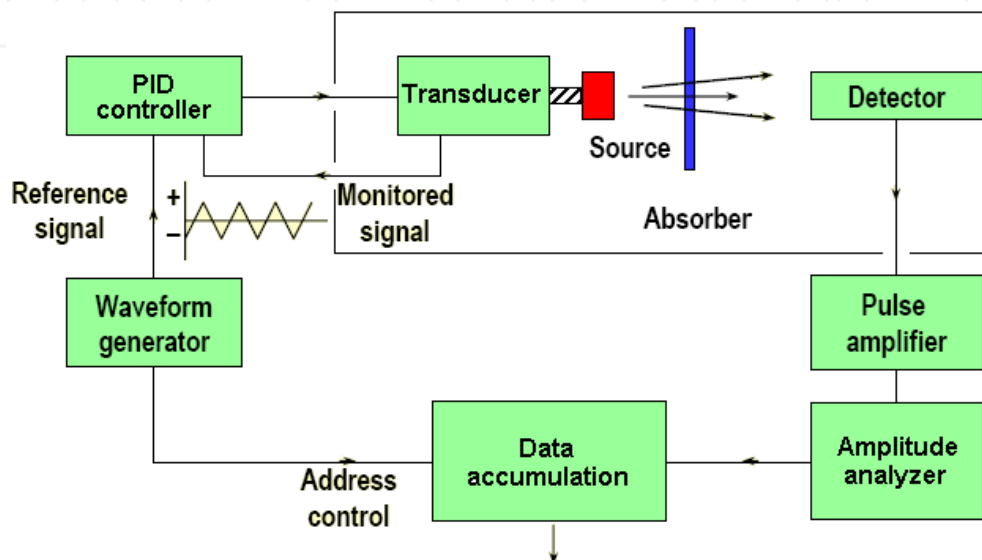


Fig. 21. Block diagram of the standard Mössbauer spectrometer.

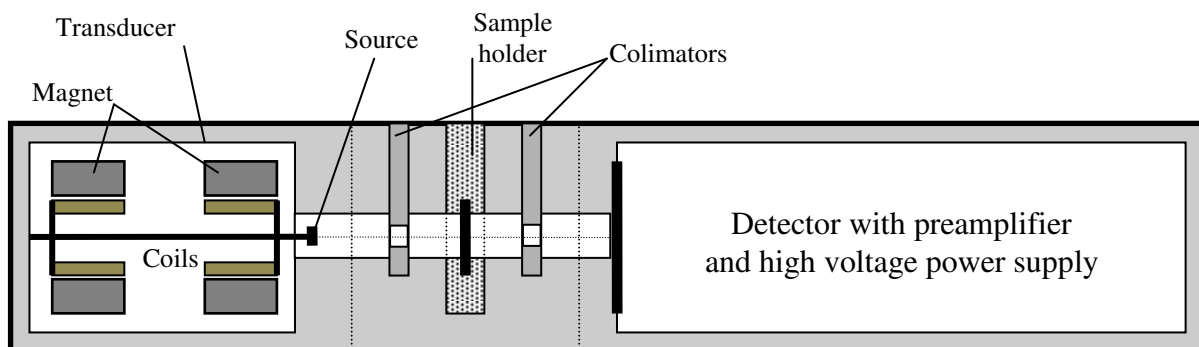


Fig. 22. Block diagram of the Mössbauer spectrometer

Various programming techniques and instrument solutions are used to develop Mössbauer spectrometers. However, traditional solutions are based primarily on stand-alone instruments or specific modular systems.

The spectrometer has to perform tasks such as  $\gamma$ -ray pulse-height analysis, reference velocity signal generation for the motion of the radioactive source, proportional integral derivative (PID) control of the relative velocity between the source and the absorber, and Mössbauer spectra accumulation. By using LabVIEW with NI PXI, PCI, USB devices, and CompactRIO, a Mössbauer spectrometer that is open and flexible enough to operate within multiple hardware setups was built (Pechousek et al., 2010).

4.2 Amplitude analyzer and spectra accumulation

The system’s  $\gamma$ -ray detector and amplitude analyzer are based on an NI high-speed digital oscilloscope. The detector impulses represent registered nuclear events, the amplitude of which depends on the detected  $\gamma$  photon energy. The sampling rate of the detector output signal differs with the detector type (scintillation, gas-filled, semiconductor). The detection function was performed using NI PXI, PCI, and USB digitizers; the NI 5102 8-bit 20 MS s<sup>-1</sup> modules, NI PCI-5124 12-bit 200 MS s<sup>-1</sup> high-resolution digitizer, and NI USB-5133 8-bit 100 MS s<sup>-1</sup> digitizer/oscilloscope.

The spectra accumulation process combines the radioactive source velocity data with the corresponding  $\gamma$ -ray intensity. Only some emitted photons with appropriate energy are affected by the specimen, and only relevant impulses are identified and recorded. The amplitude discriminator is based on the LabVIEW WPKD function. The other software component performs the multichannel analysis of the detector signal.

Figure 23 shows the basic concept of the spectrometer block diagram. This code synchronizes the DAQ process for the velocity signal generation and the detector signal processing.

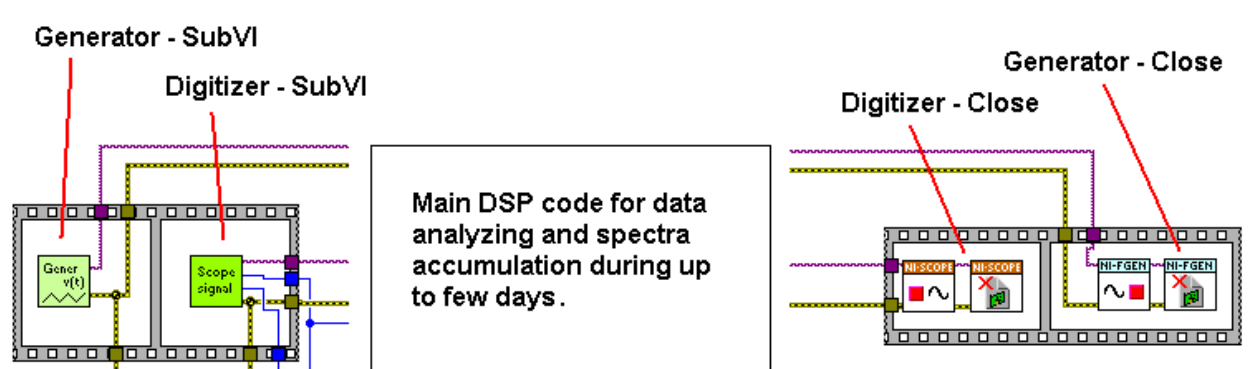


Fig. 23. The basic concept of the spectrometer block diagram..

Other SubVIs for data handling, measurement configuration, etc. are included in the application. The front panel of the main application is shown in Figure 24.

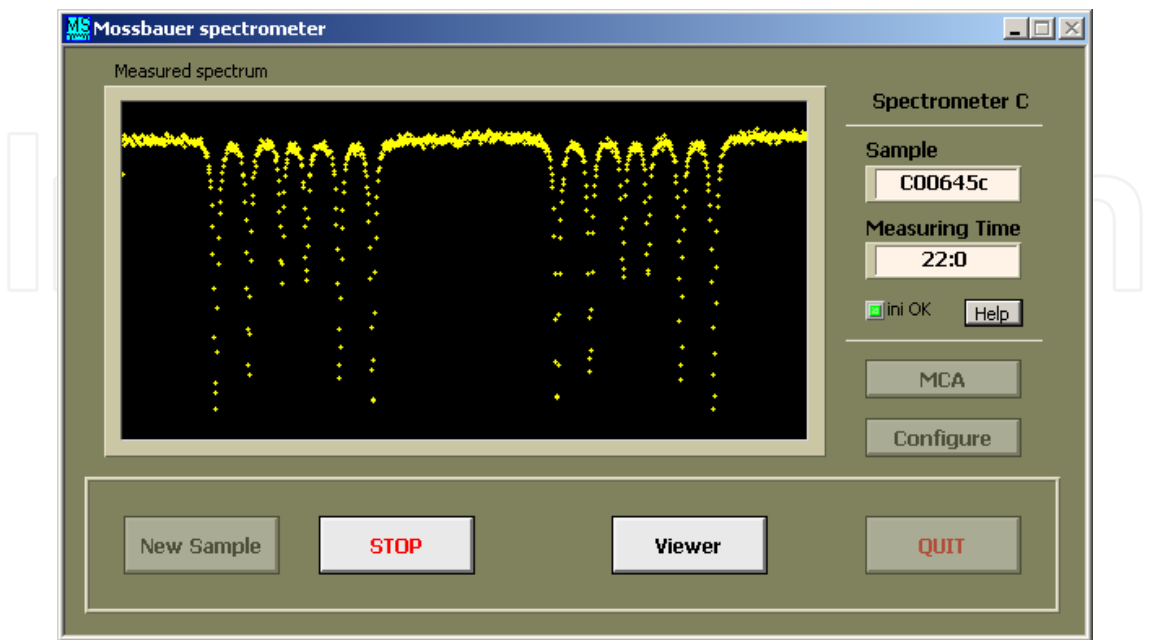


Fig. 24. Main application front panel.

### 4.3 Velocity-driving system

A common velocity-driving system for Mössbauer spectrometer consists of the velocity signal generator, PID controller, and the electromechanical linear transducer coupled with the Mössbauer source. The reference signal is lead through a PID controller to the drive coil of the transducer, and the pick-up coil signal is connected back into the PID controller. The common reference velocity a), drive b), and error c) signals are presented in Figure 25. The velocity signal frequency is mostly up to tens of Hz.

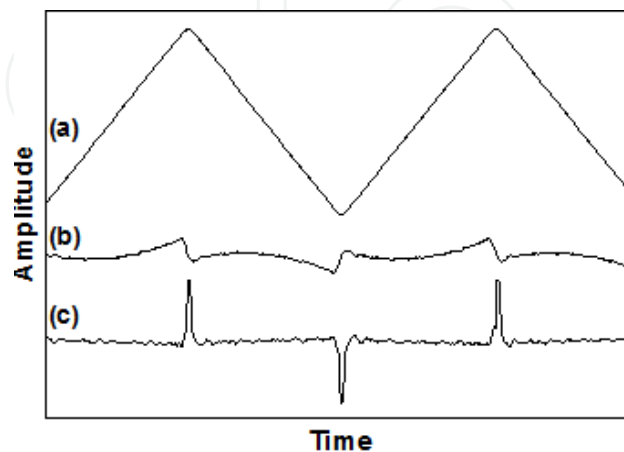


Fig. 25. Velocity a), drive b), and error c) signals used in the velocity unit.

NI analog output devices as velocity signal generators are coupled to the digital PID circuit. In addition, with the flexibility of the VI concept, generator can be replaced by the other multifunction card with proper analog and digital output on the USB, PCI or PXI platform. Limiting parameters are 12-bit resolution and the  $150 \text{ kS s}^{-1}$  update rate at the analog output as the minimum. The selected devices are for instance the NI USB-6221 16-bit  $833 \text{ kS s}^{-1}$  and NI USB-6215 16-bit  $250 \text{ kS s}^{-1}$  multifunction DAQ modules. One advantage of using PXI and PCI modules is that the RTSI bus allows transferring of fast trigger signals, which must be generated to synchronize the spectra accumulation process.

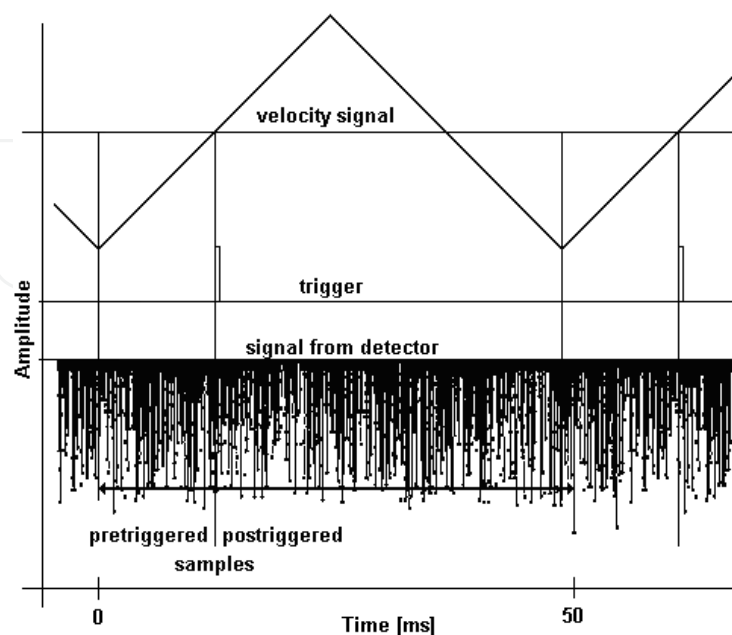


Fig. 26. DAQ processes synchronization.

In Figure 26, the basic principle of the DAQ processes synchronized with the techniques described above is depicted. The velocity signal is generated with given frequency and the trigger signal synchronizes the detector signal acquisition.

Each period of the source movement is divided into 2048 velocity/time intervals. The number of the detected photons accumulated during each time interval is saved into the relevant velocity channel. The spectra accumulation process is based on the periodical summation of the appropriate data from each repetitive movement period for hours or days. The spectra accumulation process is depicted in Figure 27.

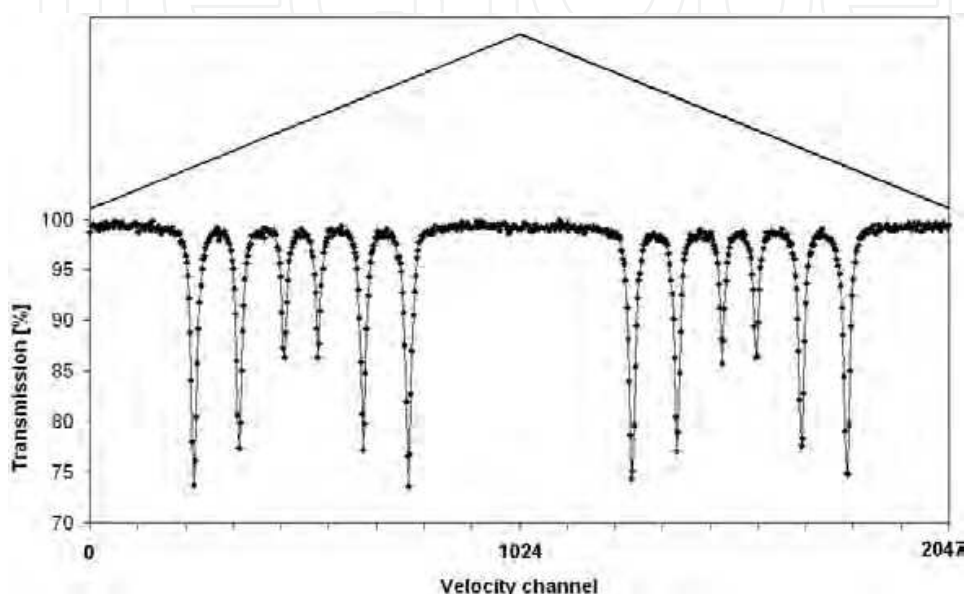


Fig. 27. Mössbauer spectrum accumulation

For the second available generator, NI CompactRIO was selected to build a digital PID controller and the reference velocity generator in the joint device (Pechousek et al., 2009). The cRIO real-time controller and cRIO chassis with an FPGA provide the digital PID algorithm based on discrete PID function in the LabVIEW FPGA Module. The analog input module acquires the transducer pick-up coil signal and the reference velocity signal when an external generator is used. The analog output module generates the drive signal, and the digital output module is used as a trigger source.

#### 4.4 Spectrometer utilization

Currently, at the Regional Centre of Advanced Technologies and Materials, a part of Palacky University in Olomouc ([www.rcptm.com](http://www.rcptm.com)), three VI spectrometers based on USB (multifunction card and high-rate digitizer), PCI (function generator and high-rate digitizer) and PXI (function generator and high-rate digitizer in the NI PXI-1033 5-slot chassis with integrated MXI-Express controller) are used.

The new digital PID system based on CompactRIO is used in the most important application in which it has achieved higher stability and system reliability in nonstandard working conditions, including vibrations coming from lab equipment and external magnetic forces. CompactRIO serves as a remote system, which allows to change the PID parameters at a safe distance from the radioactive source and the high magnetic field.

## 5. Conclusion

The measurement systems built with LabVIEW modular instrumentation offer a popular approach to nuclear spectrometers construction. By replacing the former single-purpose system units with universal data acquisition modules, it is achieved a lower-cost solution that is reliable, fast, and takes high-quality measurements. The result is a user-friendly application with high system flexibility.

Performances of the DSP systems were directly determined by spectroscopy application. The presented methods are simple in realization simultaneously with improvement in performance for nuclear experiments. Moreover, with VI open approach, it is easy to modify the configuration of the system in the future.

## 6. Acknowledgment

This work has been supported by the projects “Advanced Technologies in the Study of Applied Physics” (CZ.1.07/2.2.00/07.0018) and “Education of Research Workers in the Regional Centre of Advanced Technologies and Materials” (CZ.1.07/2.3.00/09.0042) in Operational Program Education for Competitiveness - European Social Fund. Author would also like to thank to Karolina Siskova for her help with this paper.

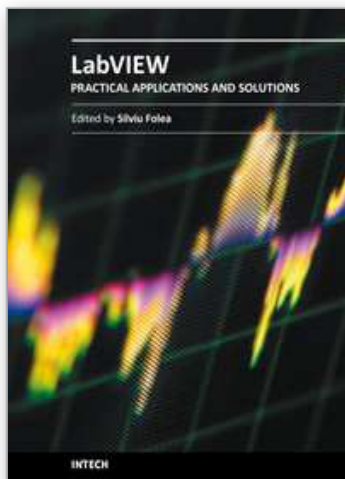
## 7. References

- Abdel-Aal, R.E. (1993). Simulation and analysis of nuclear physics instrumentation using the LabVIEW graphical programming environment. *The Arabian Journal for Science and Engineering*, Vol. 18, No. 3, (July 1993), pp. 365-382, ISSN 1319-8025
- Ahmed, S.N. (2007). *Physics and Engineering of Radiation Detection* (first edition), Academic Pres, ISBN 0-12-045581-1, London, Great Britain
- Aspinall, M.D., Joyce, M.J., Mackin, R.O., Jarrah, Z., Boston, A.J., Nolan, P.J., Peyton, A.J. & Hawkes, N.P. (2009). Sample-interpolation timing: an optimized technique for the digital measurement of time of flight for  $\gamma$  rays and neutrons at relatively low sampling rates. *Measurement Science and Technology*, Vol. 20, (November 2008), 015104, 10pp, ISSN 0957-0233
- Belli, F., Esposito, B., Marocco, D., Riva, M., Kaschuk, Y., Bonheure, G. & JET EFDA contributors (2008). A method for digital processing of pile-up events in organic scintillators. *Nuclear Instruments and Methods in Physics Research A*, Vol. 595, (July 2008), pp. 512-519, ISSN 0168-9002
- Bettiol, A.A., Udalagama, C. & Watt, F. (2009). A New Data Acquisition System for Nuclear Microscopy based on a Field Programmable Gate Array Card. *Nuclear Instruments and Methods in Physics Research B*, Vol. 267, (June 2009), pp. 2069-2072, ISSN 0168-583X
- Cosulich, E. & Gatti, F. (1992). A digital processor for nuclear spectroscopy with cryogenic detectors. *Nuclear Instruments and Methods A*, Vol. 321, (September 1992), pp. 211-215, ISSN 0168-9002
- Dickson, D.P.E. & Berry, F.J. (1986) *Mössbauer spectroscopy*. Cambridge: Cambridge University press, ISBN 978-0521018104
- Drndarević, V. (2008). A very low-cost alpha-particle spectrometer. *Measurement Science and Technology*, Vol. 19, (April 2008), 057007, 5pp, ISSN 0957-0233



- Drndarevic, V. & Jevtic, N. (2008). A versatile, PC-based gamma ray monitor. *Radiation Protection Dosimetry*, Vol. 129, No. 4, (October 2007), pp. 478-480, ISSN 1742-3406
- Ellis, W.H. & He, Q. (1993). Computer-Based Nuclear Radiation Detection and Instrumentation Teaching Laboratory System. *IEEE Transactions on Nuclear Science*, Vol. 40, No. 4, (August 1993), pp. 675-679, ISSN 0018-9499
- Esposito, B., Riva, M., Marocco D. & Kaschuck Y. (2007). A Digital Acquisition and Elaboration System for Nuclear Fast Pulse Detection. *Nuclear Instruments and Methods in Physics Research A*, Vol. 572, (March 2007), pp. 355-357, ISSN 0168-9002
- Gilmore, G. (2008). *Practical Gamma-ray Spectroscopy* (second eddition), Wiley, ISBN 978-0470861967,
- Gontean, A. & Szabó, R. (2011). LabVIEW Remote Lab, In: *LabVIEW - Modeling, Programming and Simulations*, Riccardo de Asmundis, ISBN 978-953-307-521-1, InTech, Rijeka, Croatia
- Green, D.P., Bruce J.B. & Thomas, J.L. (1996). Sensor Measurement and Experimental Control in Nuclear Magnetic Resonance Imaging. *Review of Scientific Instruments*, Vol. 67, No. 1, (January 1996), pp. 102-107, ISSN 0034-6748
- Kholmetskii, A.L., Mashlan, M., Misevich, O.V., Chudakov, V.A., Lopatik, A.R. & Zak, D. (1997). Comparison of the productivity of fast detectors for Mössbauer spectroscopy. *Nuclear Instruments and Methods in Physics Research B*, Vol. 124, (April 1997), pp. 143-144, ISSN 0168-583X
- Kirichenko, A.F., Sarwana, S., Mukhanov O.A., Vernik I.V., Zhang, Y., Kang, J. & Vogt, J.M. (2001). RSFQ Time Digitizing System. *IEEE Transactions on Applied Superconductivity*, Vol. 22, No. 1, (March 2001), pp. 978-981, ISSN 1051-8223
- Krasilnikov, V., Marocco, D., Esposito, B., Riva, M. & Kaschuck, Y. (2011). Fast pulse detection algorithms for digitized waveforms from scintillators. *Computer Physics Communications*, Vol. 182, (October 2010), pp. 735-738, ISSN 0010-4655
- Moreno, E., Reyes, P. & de la Rosa, J.M. (2011). Time-resolved fluorescence spectroscopy with LabView, In: *LabVIEW - Modeling, Programming and Simulations*, Riccardo de Asmundis, ISBN 978-953-307-521-1, InTech, Rijeka, Croatia
- National Instruments. (2004). NI-FGEN Instrument Driver Quick Reference, 02.04.2011, Available from <http://www.ni.com/pdf/manuals/371307e.pdf>
- National Instruments. (2009). NI High-Speed Digitizers Help, 02.04.2011, Available from <http://digital.ni.com/manuals.nsf/websearch/349CC538026ACD5A862576E8004DB89D?OpenDocument&seen=1>
- National Instruments. (2009). NI Signal Generators Help, 02.04.2011, Available from <http://digital.ni.com/manuals.nsf/websearch/6F0CB519A713D1E28625762000689402>
- National Instruments. (2010). Getting Started with NI-SCOPE, 02.04.2011, Available from <http://zone.ni.com/devzone/cda/tut/p/id/3382>
- Nelson, M.A., Rooney, B.D., Dinwiddie, D.R. & Brunson, G.S. (2003). Analysis of digital timing methods with BaF2 scintillators. *Nuclear Instruments and Methods in Physics Research A*, Vol. 579, (June 2003), pp. 247-251, ISSN 0168-9002
- Pechousek, J. & Mashlan, M. (2005). Mössbauer spectrometer in the PXI/CompactPCI modular system. *Czechoslovak Journal of Physics*, Vol. 55, No. 7, (July 2005), pp. 853-863, ISSN 0011-4626

- Pechousek, J., Mashlan, M., Frydrych, J., Jancik, D. & Prochazka, R. (2007). Improving detector signal processing with Pulse Height Analysis in Mössbauer Spectrometers. *Hyperfine Interactions*, Vol. 107, (February 2007), pp. 1-8, ISSN 0304-3843
- Pechousek, J., Prochazka, R., Mashlan, M., Jancik, D. & Frydrych, J. (2009). Digital proportional-integral-derivative controller of a Mössbauer Spectrometer. *Measurement Science and Technology*, Vol. 20, (November 2008), 017001, 4pp, ISSN 0957-0233
- Pechousek, J., Jancik, D., Evdokimov, V. & Prochazka, R. (2009). Velocity driving system for an in-field Mössbauer spectrometer. *Nuclear Instruments and Methods in Physics Research B*, Vol. 267, (February 2009), pp. 846-848, ISSN 0168-583X
- Pechousek, J., Prochazka, R., Jancik, D., Mashlan, M. & Frydrych, J. (2010). Universal LabVIEW-powered Mössbauer spectrometer based on the USB, PCI or PXI devices. *Journal of Physics: Conference Series*, Vol. 217, (May 2010), pp. 012006, ISSN 1742-6588
- Pechousek, J., Prochazka, R., Prochazka, V. & Frydrych, J. (2011). Virtual instrumentation technique used in the nuclear digital signal processing system design: Energy and time measurement test. *Nuclear Instruments and Methods in Physics Research A*, Vol. 637, (February 2011), pp. 200-205, ISSN 0168-9002
- Prochazka, R., Tucek, P., Tucek, J., Marek, J., Mashlan, M. & Pechousek, J. (2010). Statistical analysis And digital processing of the Mössbauer spectra. *Measurement Science and Technology*, Vol. 21, (January 2010), 025107, 7pp, ISSN 0957-0233
- Tłaczala, W., Grajner, G. & Zaremba, M. (2008). Virtual Laboratory with Simulated Nuclear Experiments. *IEEE Transactions on Instrumentation and Measurement*, Vol. 57, No. 8, (August 2008), pp. 1766-1770, ISSN 0018-9456
- Tłaczala, W. (2005). Virtual instrumentation in physics, In: *Handbook of Measuring System Design*, P. Sydeman & R. Thorn, (Eds.), 695-701, Wiley, ISBN 0-470-02143-8, Hoboken, NJ, USA
- Yan, J., Liu, R., Li, Ch., Jiang, L., Lu, X., Zhu, T., Wang, M., Wen, Z. & Lin, J. (2009). LabVIEW-based auto timing counts virtual instrument system with ORTEC 974 Counter/Timer. *Nuclear Science and Techniques*, Vol. 20, (October 2009), pp. 307-311, ISSN 1001-8042
- Yang, H., Wehe, D.K. & Bartels, D.M. (2009). Spectroscopy of high rate events during active interrogation. *Nuclear Instruments and Methods in Physics Research A*, Vol. 598, (October 2008), pp. 779-787, ISSN 0168-9002



## **Practical Applications and Solutions Using LabVIEW™ Software**

Edited by Dr. Silviu Folea

ISBN 978-953-307-650-8

Hard cover, 472 pages

**Publisher** InTech

**Published online** 01, August, 2011

**Published in print edition** August, 2011

The book consists of 21 chapters which present interesting applications implemented using the LabVIEW environment, belonging to several distinct fields such as engineering, fault diagnosis, medicine, remote access laboratory, internet communications, chemistry, physics, etc. The virtual instruments designed and implemented in LabVIEW provide the advantages of being more intuitive, of reducing the implementation time and of being portable. The audience for this book includes PhD students, researchers, engineers and professionals who are interested in finding out new tools developed using LabVIEW. Some chapters present interesting ideas and very detailed solutions which offer the immediate possibility of making fast innovations and of generating better products for the market. The effort made by all the scientists who contributed to editing this book was significant and as a result new and viable applications were presented.

### **How to reference**

In order to correctly reference this scholarly work, feel free to copy and paste the following:

Jiri Pechousek (2011). Application of Virtual Instrumentation in Nuclear Physics Experiments, Practical Applications and Solutions Using LabVIEW™ Software, Dr. Silviu Folea (Ed.), ISBN: 978-953-307-650-8, InTech, Available from: <http://www.intechopen.com/books/practical-applications-and-solutions-using-labview-software/application-of-virtual-instrumentation-in-nuclear-physics-experiments>

**INTECH**  
open science | open minds

### **InTech Europe**

University Campus STeP Ri  
Slavka Krautzeka 83/A  
51000 Rijeka, Croatia  
Phone: +385 (51) 770 447  
Fax: +385 (51) 686 166  
[www.intechopen.com](http://www.intechopen.com)

### **InTech China**

Unit 405, Office Block, Hotel Equatorial Shanghai  
No.65, Yan An Road (West), Shanghai, 200040, China  
中国上海市延安西路65号上海国际贵都大饭店办公楼405单元  
Phone: +86-21-62489820  
Fax: +86-21-62489821

© 2011 The Author(s). Licensee IntechOpen. This chapter is distributed under the terms of the [Creative Commons Attribution-NonCommercial-ShareAlike-3.0 License](https://creativecommons.org/licenses/by-nc-sa/3.0/), which permits use, distribution and reproduction for non-commercial purposes, provided the original is properly cited and derivative works building on this content are distributed under the same license.

IntechOpen

IntechOpen